Journal of Oceanology and Limnology

https://doi.org/10.1007/s00343-022-2017-1

A new chloro-azaphilone derivative with pro-angiogenesis activity from the hadal trench-derived fungus *Chaetomium globosum* YP-106*

Yaqin FAN[1, 2, #], Chunjiao JIANG[2, #], Peihai LI[3], Cong WANG[4, **], Hao CHEN[1, **]

[1] *MNR Key Laboratory of Marine Eco-Environmental Science and Technology, First Institute of Oceanography, Ministry of Natural Resources, Qingdao 266061, China*

[2] *Shandong Provincial Key Laboratory of Applied Mycology, School of Life Sciences, Qingdao Agricultural University, Qingdao 266109, China*

[3] *Engineering Research Center of Zebrafish Models for Human Diseases and Drug Screening of Shandong Province, Shandong Provincial Engineering Laboratory for Biological Testing Technology, Key Laboratory for Biosensor of Shandong Province, Biology Institute, Qilu University of Technology (Shandong Academy of Sciences), Jinan 250103, China*

[4] *Key Laboratory of Chemistry and Engineering of Forest Products, State Ethnic Affairs Commission, Guangxi Key Laboratory of Chemistry and Engineering of Forest Products, Guangxi Collaborative Innovation Center for Chemistry and Engineering of Forest Products, School of Chemistry and Chemical Engineering, Guangxi Minzu University, Nanning 530006, China*

Received Jan. 22, 2022; accepted in principle Mar. 4, 2021; accepted for publication Mar. 8, 2022

Abstract A new chloro-azaphilone derivative chaetoviridin L (**1**) along with four known analogues, namely, chaetomugilin A (**2**), chaetoviridin E (**3**), chaetomugilin O (**4**), and chaephilone D (**5**), is isolated and identified from the culture extract of *Chaetomium globosum* YP-106, a deep-sea derived fungus obtained from the hadal zone seawater collected in the Yap Trench. Their structures were determined based on detailed interpretation of nuclear magnetic resonance (NMR) spectroscopic, mass spectrometry (MS) data analysis and comparison with the reported literature. The absolute configuration of the new compound was established by quantum chemical calculations of electronic circular dichroism (ECD). All the isolated compounds were evaluated for pro-angiogenesis activity using zebra fish model. Compounds **1**, **2**, and **5** significantly promoted the angiogenesis in a dose-dependent manner and thus, these compounds might be used as promising molecules for the treatment of cardiovascular disease.

Keyword: marine natural products; marine-derived fungi; azaphilones; hadal trench; deep-sea; *Chaetomium globosum*; pro-angiogenesis activity

1 INTRODUCTION

The hadal zones are composed of trenches with a water depth of more than 6 000 m, occupying 45% of the deep-sea region (Sanei et al., 2021; Weston et al., 2021). Those areas have become the most unique habitats in the deep sea because of low oxygen, low temperature, high pressure, and no light. In these extreme environments, hadal fungi gradually evolved to with stand those harsh conditions by changing their corresponding physiological characteristics, genetic mechanism, and metabolic systems. Thus, they are considered as relatively underexploited resources of novel bioactive compounds (Chen et al., 2021). Recently, deep-sea fungi have been recognized as important sources of novel active secondary metabolites with anticancer (Zhang et al., 2020), antimicrobial (Niu et al., 2021), anti-inflammatory (Guo et al., 2021), and other biological activities (Wang et al., 2020; Chi et al., 2021).

* Supported by the National Natural Science Foundation of China (No. 42006096), the Shandong Provincial Natural Science Foundation (No. ZR2020QD098), and the China Postdoctoral Science Foundation (No. 2020M682266)

** Corresponding authors: wangcong123206@163.com; hchen@fio.org.cn

# Yaqin FAN and Chunjiao JIANG contributed equally to this work and should be regarded as co-first authors.

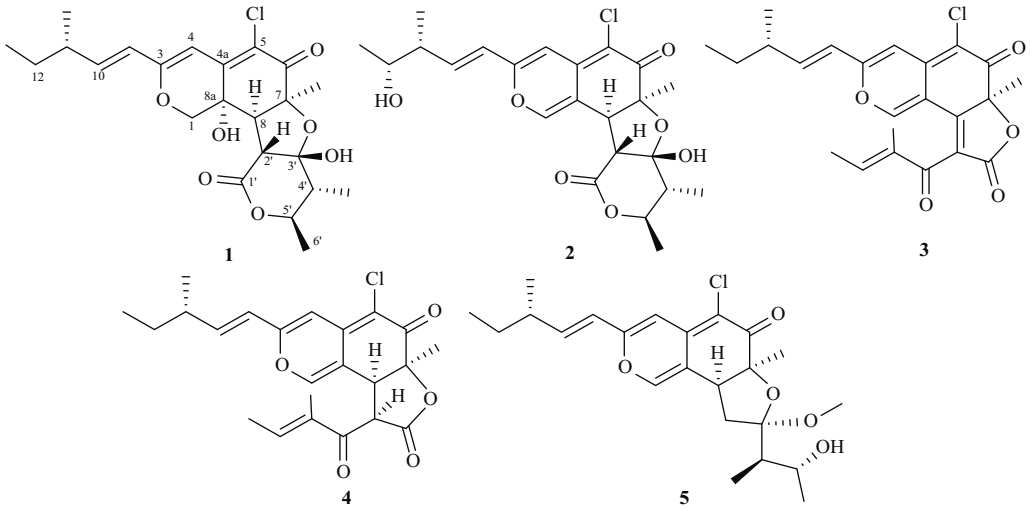

Fig.1 The chemical structures of Compounds 1–5

Compound **1**: chaetoviridin L; Compound **2**: chaetomugilin A; Compound **3**: chaetoviridin E; Compound **4**: chaetomugilin O; Compound **5**: chaephilone D.

Cardiovascular disease is the leading cause of death in mankind. Among cardiovascular diseases, ischemic heart disease and stroke are the most common and harmful, accounting for 85% of global cardiovascular deaths (Writing Group Members et al., 2009; GBD 2017 Causes of Death Collaborators, 2018). Angiogenesis therapy can achieve the therapeutic effect of cardiovascular disease by the means of blood supply reconstruction and blood supply insufficiency improving (Carmeliet and Jain, 2011). As a new target for cardiovascular drug development, pro-angiogenesis has attracted increasing attention (Gut et al., 2017).

In our continuous efforts for searching and screening for novel secondary metabolites with pro-angiogenic activity (Fan et al., 2015), a fungal strain of *Chaetomium globosum* YP-106 was isolated from the hadal zone seawater collected at a depth of 6 215 m from Yap Trench in the western Pacific Ocean. Chemical investigation of the fungus resulted a group of chloro-azaphilone derivatives, including one previously undescribed chloro-azaphilone derivative, chaetoviridin L (**1**), together with four related known azaphilones, chaetomugilin A (**2**) (Yamada et al., 2008), chaetoviridin E (**3**) (Phonkerd et al., 2008), chaetomugilin O (**4**) (Muroga et al., 2009), and chaephilone D (**5**) (Gao et al., 2020) (Fig.1). All isolated compounds were tested for pro-angiogenic activities in zebrafish model. Compounds **1**, **2**, and **5** (at concentrations of 20 μg/mL, 40 μg/mL, and 80 μg/mL) significantly promoted the pro-angiogenesisin a dose-dependent manner. This is the first report of the azaphilones displayed pro-angiogenesis activities. Here in we report the isolation, structural elucidation, and biological evaluation of Compounds **1**–**5**.

2 MATERIAL AND METHOD

2.1 General experimental procedure

Optical rotations were measured with a MCP 500 automatic polarimeter (Anton Paar) with $CHCl_3$ as solvent. Ultraviolet (UV) spectra were recorded on V-550 UV/vis spectrophotometer. Electronic circular dichroism (ECD) spectra were measured on JASCO J-815 spectrometer. ^{1}H, ^{13}C nuclear magnetic resonance (NMR), distortionless enhancement by polarization transfer (DEPT), and 2D NMR spectra were recorded on a Bruker Avance 600 spectrometer (Bruker). High resolution electrospray ionization mass spectroscopy (HRESIMS) spectra were recorded using the quadrupole-time of flight (Q-TOF) ULTIMA GLOBAL GAA076 LC mass spectrometer. Thin layer chromatography (TLC) was performed on plates precoated with silica gel GF 254 (10–40 μm) and silica gel (200–300 mesh) (Qingdao Haiyang Chemical Co., Qingdao, China). Vacuum-liquid chromatography (VLC) used silica gel H (Qingdao Marine Chemical Factory). Sephadex LH-20 (Pharmacia Biotec AB, Uppsala, Sweden), and reverse-phase C18 silica gel (Merck, Darmstadt, Germany) were used for column chromatography (CC). All solvents used were of analytical grade (Sinopharm Chemical Reagent Co., Shanghai, China). Semi-preparative high performance liquid chromatography (HPLC) was performed using an octadecylsilyl (ODS) column (YMC-pack ODS-A, 10 mm×250 mm, 5 μm, 4.0 mL/min).

2.2 Fungal material

The fungus *C. globosum* YP-106 was isolated from

Table 1 The NMR data of Compound 1 in DMSO-d_6

No.	δc, type[a]	δ_H (*J* in Hz)[b]
1	73.5, CH_2	4.16 (1H, d, 12.3); 4.29 (1H, d, 12.3)
3	160.3, C	
4	100.7, CH	6.05, s
4a	143.4, C	
5	120.9, C	
6	189.2, C	
7	83.3, C	
8	55.4, CH	2.67 (1H, d, 9.1)
8a	67.5, C	
9	123.0, CH	6.20 (1H, d, 15.8)
10	144.5, CH	6.40 (1H, dd, 15.8,7.9)
11	37.9 CH	2.22 (1H, dq, 13.7, 6.8)
12	28.7, CH_2	1.36 (2H, dq, 14.2, 7.2)
13	11.6, CH_3	0.85 (3H, t, 7.4)
7-Me	25.2, CH_3	1.54 (3H, s)
11-Me	19.3, CH_3	1.02 (3H, d, 6.7)
1′	171.4, C	
2′	54.6, CH	2.80 (1H, d, 9.1)
3′	103.6, C	
4′	44.5, CH	1.69 (1H, dq, 13.9, 6.3)
5′	76.7, CH	4.30 (1H, dd, 13.9, 6.3)
6′	18.5, CH_3	1.25 (3H, d, 6.4)
4′-Me	9.4, CH_3	0.93 (3H, d, 6.4)
3′-OH		6.23, s
8a-OH		6.03, s

[a]: measured at 125 MHz; [b]: measured at 600 MHz; both [a] and [b] are measured in Dimethyl Sulfoxide (DMSO)-d_6. δ in $\times 10^{-6}$; *J* in Hz.

a marine seawater sample collected in November, 2017, from the Yap Trench of the Pacific Ocean at a depth of 6 215 m. The fungus was identified using a molecular biological protocol by DNA amplification and sequencing of the ITS region. The BLAST sequence was deposited in the NCBI GenBank under the accession No. OL872214. This strain has been preserved at MNR Key Laboratory of Marine Eco-Environmental Science and Technology, First Institute of Oceanography, Ministry of Natural Resources, China.

2.3 Fermentation, extraction, and isolation

The fungus *C. globosum* YP-106 was aseptically inoculated into fifty 1-L conical flasks, and cultured at 28 °C for 30 days. Each flask contains 300 mL of liquid nutrient medium which is composed of malt extract (17 g/L), glucose (3 g/L), peptone (3 g/L), sea salt (33 g/L) and tap water. After fermentation and filtering the entire broth (15 L), the broth medium was extracted with ethyl acetate (EtOAc) and the solid mycelia were extracted with 85% volume of aqueous acetone. Mixed extracts of fermentation broth and mycelium (35 g) were eluted by a stepwise gradient of petroleum ether (EtOEt):ethyl acetate (EtOAc) (80∶1, 50∶1, 20∶1, 10∶1, 8∶1, 6∶1, 2∶1, and 1∶1 by volume, 1 L each) and chloroform (CHCl3): methanol (MeOH) (50∶1, 20∶1, 10∶1, 5∶1, 1∶1, and 0∶1, by volume, 1 L each). Six fractions (Fr.1−Fr.6) were separated and obtained by passing through silica gel (200−300 mesh) VLC columns. Among them, Fr.2 (5.8 g) was further purified by CC on Sephadex LH-20 using 100% MeOH to give eight subfractions of Fr.2.1–Fr.2.8. Subfraction 2.3 was further subjected to HPLC purification using ODS column (MeOH-H_2O, 80∶20 by volume) to yield Compound **4** (7.2 mg). More over Subfraction 2.4 was purified by HPLC eluting with isocratic isocratic 45∶55 MeOH-H_2O to yield Compound **1** (1.8 mg). Fraction 3 (0.8 g) was further separated into six subfractions by reversed phase ODS using stepwise gradient elution with MeOH/H_2O (10%–100%). Subfraction 3.5 was further purified by Sephadex LH-20 CC using 100% MeOH and then followed by HPLC (MeCN-H_2O, 75∶25 by volume) to yield Compound **3** (1.1 mg). Gradient elution of MeOH/H_2O (10%–100%) of Fr.4 (2.5 g) was further separated by CC on RP-18 eluting with MeOH-H_2O gradients (10%−100%) to yield six subfractions (Fr.4.1–Fr.4.6). Subfraction 4.5 was purified by Sephadex LH-20 CC eluted with 100% MeOH and further purification using HPLC on ODS (MeOH-H_2O, isocratic 45∶55 by volume) to yield Compound **5** (1.1 mg). Fr.5 (3.8 g) was eluted by MeOH/H_2O (10%–100%) in a step-by-step gradient with ODS as filler to obtain three subfractions Fr.5.1 –Fr.5.3. Subfraction 5.2 was eluted with Sephadex LH-20 CC using 100% MeOH and then semi-prepared with HPLC (MeCN-H_2O, 35∶65 volume) to obtain Compound **2** (1.1 mg).

2.4 Spectral data

Chaetoviridin L (**1**): yellow amorphous powder; [α]25 D-26 (*c* 0.19, $CHCl_3$); UV (MeOH) λ_{max} 239 (4.9), 296 (4.8), and 375 (5.6) nm; CD (*c* 0.1, MeOH) λ_{max} ($\Delta\varepsilon$) 211 (-2.6), 242 (+1.1), 259 (-0.3), 327 (+0.2), and 390 (-2.5) nm; ^{1}H and^{13}C NMR data, see Table 1; HRESIMS *m*/*z* 453.168 4 $[M+H]^+$ (calcd for $C_{23}H_{30}O_7Cl$, 453.167 5).

2.5 Pro-angiogenic activity experiment

Male and female zebrafish (Transgenic zebrafish): Tg (flk1:EGFP) were raised under conditions of a 14-h light/10-h dark cycle, separately. Healthy male and female mature zebrafish were placed in the breeding tank at a ratio of 1:1 during egg collection, and fertilized eggs were obtained at the next morning. After disinfection and washing, the fertilized eggs were transferred to zebrafish embryo culture water (containing 5.0-mmol/L NaCl, 0.17-mmol/L KCl, 0.4-mmol/L $CaCl_2$, and 0.16-mmol/L $MgSO_4$), and cultured at 28±0.5 °C under controlled light for 24 h. The egg membranes were removed with 1-mg/mL protease E solution. The pro-angiogenesis activities of Compounds **1**–**5** were evaluated in the zebrafish model with vascular defects induced by vatalanib (PTK787, Basel, Switzerland). The test compounds (20, 40, and 80 μg/mL) and 0.2-μg/mL PTK787 were added in the 24-well plates with zebrafish embryos (n=10/well), as well as 10-μL/mL danhong as the positive control. After incubation in a light-operated incubator at 28.0 °C for 24 h, the number of intersegmental vessels (ISV) were collected using a fluorescence microscope (SZX16 Tokyo, Japan) (Li et al., 2021).

2.6 ECD calculation of Compound 1

Conformations were searched in HyperChem 8.0 software using the Molecular mechanical MM+ method, and geometric optimization at the gas-phase B3LYP/6-31G(d) level was performed using Gaussian09 software (Ver. D.01; Gaussian, Inc., Wallingford, CT, USA) (Frisch et al., 2013) to afford the energy-minimized conformers. Then, the ECD spectra of the optimized conformations were calculated using time-dependent density functional theory (TD-DFT) at BH&HLYP/TZVP, CAM-B3LYP/TZVP, and PEB0/TZVP levels, and the solvent effects of MeOH solution were evaluated using SCRF/PCM method at the same DFT levels.

3 RESULT AND DISCUSSION

Compound **1** was yellow amorphous powder. In the HRESIMS spectrum, the presence of chlorine atoms in Compound **1** was inferred due to the presence of two isotopes $[M+H]^+/[M+H+2]^+$ with a peak intensity ratio of 3:1. The molecular formula of Compound **1** was established as $C_{23}H_{29}O_7Cl$ by HRESIMS peak at m/z 453.168 4 $[M+H]^+$ (Supplementary Fig.S1), which indicating 9 degrees of unsaturation. The UV

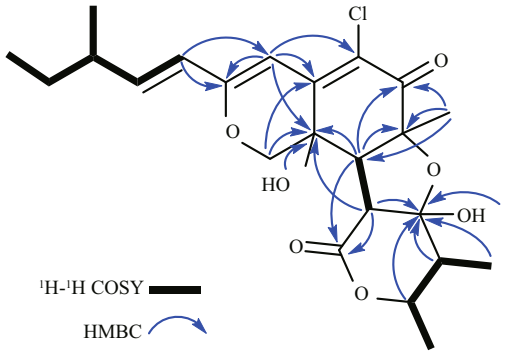

Fig.2 Key ^{1}H-^{1}H COSY and HMBC correlations of Compound 1

spectrum of Compound **1** showed characteristic absorptions for azaphilone chromophore at λ_{max} 239, 296, and 375 nm indicating a highly conjugated system. The ^{1}H-NMR (Table 1 & Supplementary Fig.S2), ^{13}C-DEPTQ (Table 1 & Supplementary Fig.S3), and HSQC (Supplementary Fig.S4) NMR spectra revealed the presence of 23 carbon atoms, which contain five methyls, two methylenes, eight methines (including three olefinic and one oxygenated) and eight quaternary carbons (containing three oxygenated, three olefinic, and two carbonyls). Extensive comparison of its 1D (Supplementary Figs. S2 & S3) and 2D data (Supplementary Figs.S4–S6) with those of chaetomugilin D (Yasuhide et al., 2008) revealed that the structures of these two compounds (**1** and chaetomugilin D) are very similar, except for the signals of an olefinic methine ($\delta_{C/H}$ 145.6/7.28) and an olefinic quaternary carbon (δ_C 114.3), which are absent in chaetomugilin D. In contrast, a methylene (δ_C 73.5/δ_H 4.16, 4.29) and an oxygenated carbon (δ_C 67.5) appear in the NMR spectra of **1**. These results indicated that Compound **1** was the C-1 hydrogenated and 8a-hydroxylated derivative of chaetomugilin D. This deduction was further supported by the key heteronuclear multiple bond coherence (HMBC) (Fig.2 & Supplementary Fig.S6) correlations from H-1 to C-4a and C-8a, and from H-4, H-8, H-2′, and 8a-OH to C-8a. The overall planar structure of **1** was finally defined by the HMBC and ^{1}H-^{1}H COSY correlations as shown in Fig.2.

From the large coupling constant of $J_{9/10}$=15.8 Hz in ^{1}H-NMR (Table 1 & Supplementary Fig.S2), the double-bond configuration at C-9/C-10 is pushed out to be in the *trans* form. The nuclear overhauser effect spectroscopy (NOESY) (Fig.3 & Supplementary Fig. S7) correlations from H-2′ to H-1 and H-6′, from H-6′ to H-4′ and 3′-OH indicated the cofacial orientation of these groups, while the correlations from H-8

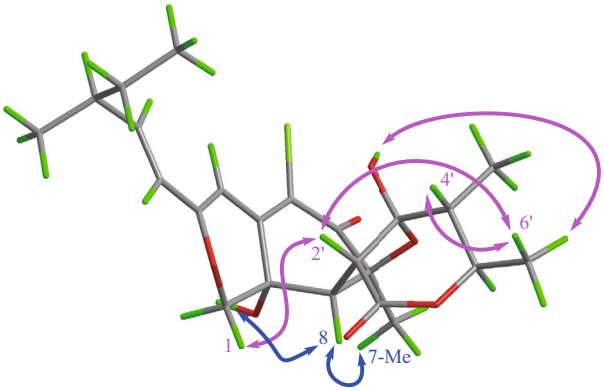

Fig.3 Key NOESY correlations for Compound 1

Blue lines: β-orientation; red lines: α-orientation.

to 7-CH_3 and 8a-OH suggested that these groups are on the opposite face. To confirm the absolute configuration of **1**, time-dependent density functional (TDDFT)-ECD calculations at three different levels were performed. The calculated ECD spectra matched well with the ECD spectra of the experimental curves, so the absolute configuration of **1** can be determined as 7*S*, 8*S*, 8a*S*, 11*S*, 2′*R*, 3′*R*, 4′*R*, 5′*R*.

The structures of known Compounds **2**–**5** were established by comparing their NMR data to the previously reported data (Phonkerd et al., 2008; Yamada et al., 2008; Muroga et al., 2009; Gao et al., 2020).

Compounds **1**–**5** (20, 40, and 80 μg/mL) were evaluated for pro-angiogenic activity in the zebrafish models. Compared with the model group, in which zebrafish's intersegmental blood vessels (ISVs) were inhibited by PTK787, Compounds **1**, **2**, and **5** showed significant vascular growth-promoting effects in a dose-dependent manner. Moreover, Compounds **1** and **2** showed stronger pro-angiogenesis activities than Compound **5** at concentrations of 40 and 80 μg/mL, Compounds **3** and **4** did not show relevant activities (Fig.5 & Supplementary Table S1). The results suggested that Compounds **1**, **2**, and **5** could be promising candidates for cardiovascular disease lead drugs. To the best of our knowledge, this is the first report for cardiovascular effects of chloro-azaphilone derivative in zebrafish.

In addition, azaphilones have been reported to be with potential applications for food colorant and ultraviolet proof products in previous report (Jongrungruangchok et al., 2004; Maciel et al., 2018). From an ecological point of view, the azaphilones isolated from deep-sea derived fungi under experimental conditions without light limitation could involve in the defense mechanism to

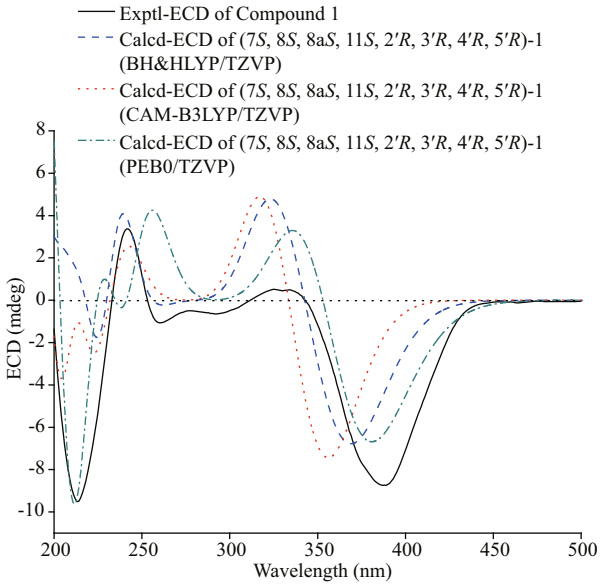

Fig.4 Experimental and calculated ECD spectra of Compound 1

avoid photodamage. These need to be confirmed by continuous in-depth studies.

4 CONCLUSION

In summary, five compounds, including a new chloro-azaphilone derivative chaetoviridin L (**1**), were obtained from the culture extract of *C. globosum* YP-106, a fungus obtained from the hadal zone seawater. The stereo-configurations of isolated compounds were determined by coupling constant, NOESY spectrum, and quantum chemical calculations of ECD. Compounds **1**, **2**, and **5** showed excellent proangiogenic activity in a dose-dependent manner, and therefore, they have the potential to be developed as natural cardiovascular disease agents.

5 DATA AVAILABILITY STATEMENT

All the data supporting the results of this study are available within the article and the supplementary material.

References

Carmeliet P, Jain R K. 2011. Molecular mechanisms and clinical applications of angiogenesis. *Nature*, **473**(7347): 298-307, https://doi.org/10.1038/nature10144.

Chen P, Zhou H, Huang Y Y et al. 2021. Revealing the full biosphere structure and versatile metabolic functions in the deepest ocean sediment of the Challenger Deep. *Genome Biology*, **22**(1): 207, https://doi.org/10.1186/s13059-021-02408-w.

Chi L P, Li X M, Wan Y P et al. 2021. Two new phenol

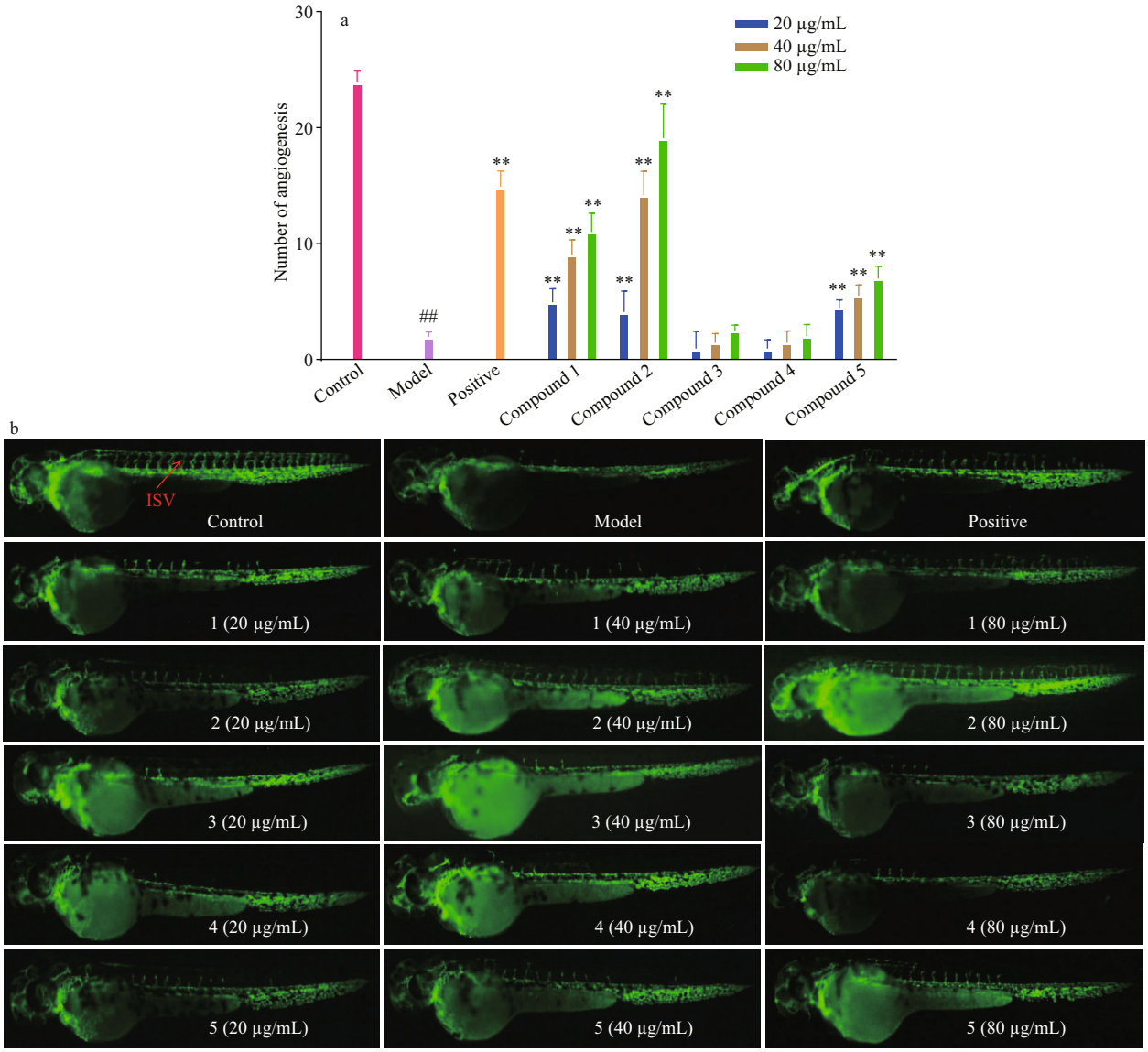

Fig.5 Vasculogenesis activity of Compounds 1−5 (20, 40, and 80 μg/mL) (a); images of intersomitic vessels (ISV) in transgenic fluorescent zebrafish (b)

##: $P<0.01$, compared with the normal control group; **: $P<0.01$, compared with the model control group.

derivatives from the cold seep-derived fungus *Aspergillus insuetus* SD-512. *Chemistry & Biodiversity*, **18**(10): e2100512, https://doi.org/10.1002/cbdv.202100512.

Fan Y Q, Li P H, Chao Y X et al. 2015. Alkaloids with cardiovascular effects from the marine-derived fungus *Penicillium expansum* Y32. *Marine Drugs*, **13**(10): 6489-6504, https://doi.org/10.3390/md13106489.

Frisch M J, Trucks G W, Schlegel H B et al. 2013. Gaussian 09, Revision D.01. Wallingford: Gaussian, Inc.

Gao W X, Chai C W, Li X N et al. 2020. Two anti-inflammatory chlorinated azaphilones from *Chaetomium globosum* TW1-1 cultured with 1-methyl-L-tryptophan and structure revision of chaephilone C. *Tetrahedron Letters*, **61**(8): 151516. https://doi.org/10.1016/j.tetlet.2019.151516

GBD 2017 Causes of Death Collaborators. 2018. Global, regional, and national age-sex-specific mortality for 282 causes of death in 195 countries and territories, 1980-2017: a systematic analysis for the Global Burden of Disease Study 2017. *The Lancet*, **392**(10159): 1736-1788, https://doi.org/10.1016/S0140-6736(18)32203-7.

Guo X, Meng Q Y, Niu S W et al. 2021. Epigenetic manipulation to trigger production of guaiane-type sesquiterpenes from a marine-derived *Spiromastix* sp. fungus with antineuroinflammatory effects. *Journal of Natural Products*, **84**(7): 1993-2003, https://doi.org/10.1021/acs.jnatprod.1c00293.

Gut P, Reischauer S, Stainier D Y R et al. 2017. Little fish, big data: zebrafish as a model for cardiovascular and metabolic disease. *Physiological Reviews*, **97**(3): 889-938, https://doi.org/10.1152/physrev.00038.2016.

Jongrungruangchok S, Kittakoop P, Yongsmith B et al. 2004. Azaphilone pigments from a yellow mutant of the fungus

Monascus kaoliang. *Phytochemistry*, **65**(18): 2569-2575, https://doi.org/10.1016/j.phytochem.2004.08.032.

Li P H, Zhang M Q, Xie D X et al. 2021. Characterization and bioactivities of phospholipids from squid viscera and gonads using ultra-performance liquid chromatography-Q-exactive orbitrap/mass spectrometry-based lipidomics and zebrafish models. *Food & Function*, **12**(17): 7986-7996, https://doi.org/10.1039/D1FO00796C.

Maciel O M C, Tavares R S N, Caluz D R E et al. 2018. Photoprotective potential of metabolites isolated from algae-associated fungi *Annulohypoxylon stygium*. *Journal of Photochemistry and Photobiology B*: *Biology*, **178**: 316-322, https://doi.org/10.1016/j.jphotobiol.2017.11.018.

Muroga Y, Yamada T, Numata A et al. 2009. Chaetomugilins I-O, new potent cytotoxic metabolites from a marine-fish-derived *Chaetomium* species. Stereochemistry and biological activities. *Tetrahedron*, **65**(36): 7580-7586. https://doi.org/10.1016/j.tet.2009.06.125.

Niu S W, Liu D, Shao Z Z et al. 2021. Chlorinated metabolites with antibacterial activities from a deep-sea-derived *Spiromastix* fungus. *RSC Advances*, **11**(47): 29661-29667, https://doi.org/10.1039/d1ra05736g.

Phonkerd N, Kanokmedhakul S, Kanokmedhakul K et al. 2008. Bis-spiro-azaphilones and azaphilones from the fungi *Chaetomium cochliodes* VTh01 and *C. cochliodes* CTh05. *Tetrahedron*, **64**(40): 9636-9645, https://doi.org/10.1016/j.tet.2008.07.040.

Sanei H, Outridge P M, Oguri K et al. 2021. High mercury accumulation in deep-ocean hadal sediments. *Scientific Reports*, **11**(1): 10970, https://doi.org/10.1038/s41598-021-90459-1.

Wang Y N, Meng L H, Wang B G. 2020. Progress in research on bioactive secondary metabolites from deep-sea derived microorganisms. *Marine Drugs*, **18**(12): 614, https://doi.org/10.3390/md18120614.

Weston J N J, Peart R A, Stewart H A et al. 2021. Scavenging amphipods from the Wallaby-Zenith Fracture Zone: extending the hadal paradigm beyond subduction trenches. *Marine Biology*, **168**(1): 1, https://doi.org/10.1007/s00227-020-03798-4.

Writing Group Members, Lloyd-Jones D, Adams R et al. 2009. Heart disease and stroke statistics—2009 update: a report from the American heart association statistics committee and stroke statistics subcommittee. *Circulation*, **119**(3): e21-e181, https://doi.org/10.1161/circulationaha.108.191261.

Yamada T, Doi M, Shigeta H et al. 2008. Absolute stereostructures of cytotoxic metabolites, chaetomugilins A-C, produced by a *Chaetomium* species separated from a marine fish. *Tetrahedron Letters*, **49**(26): 4192-4195, https://doi.org/10.1016/j.tetlet.2008.04.060.

Yasuhide M, Yamada T, Numata A et al. 2008. Chaetomugilins, new selectively cytotoxic metabolites, produced by a marine fish-derived *Chaetomium* species. *The Journal of Antibiotics*, **61**(10): 615-622, https://doi.org/10.1038/ja.2008.81.

Zhang J, Chen Y C, Liu Z M et al. 2020. Cytotoxic secondary metabolites from a sea-derived fungal strain of *Hypoxylon rubiginosum* FS521. *Chinese Journal of Organic Chemistry*, **40**(5): 1367-1371, https://doi.org/10.6023/cjoc201912012. (in Chinese with English abstract)

Electronic supplementary material

Supplementary material (Supplementary Figs.S1–S7 and Table S1) is available in the online version of this article at https://doi.org/10.1007/s00343-022-2017-1.